JES, Vol. 53, No. 4, July 2025 DOI: 10.21608/JESAUN.2025.367641.1448 Part D: Mining and Metallurgical Engineering

Journal of
Engineering Sciences
Faculty of Engineering
Assiut University
JES
مجلة
العلوم الهندسية
كلية الهندسة
جامعة أسيوط
journal homepage: http://jesaun.journals.ekb.eg

# Investigation of microstructure and corrosion behavior of friction stir welded dissimilar joints AA5754-O to AA5052-O

Received 12 March 2025; Revised 3 May 2025; Accepted 3 May 2025

**A.E. Mahmoud**[1]
**M. Abu–Okail**[2]
**I. M. Hassab-Allah**[3]
**H. Taghyan. Hussain**[4]

**Keywords**
Maritime structures,
Corrosion resistance,
Dissimilar aluminum alloys,
Process parameters of FSW,
Microstructure, Optimization

**Abstract**
The durability of maritime structures is critically affected by harsh marine environments, where saltwater exposure accelerates corrosion and compromises structural integrity. This study investigates the influence of key friction stir welding (FSW) parameters on the microstructure and corrosion behavior of dissimilar aluminum alloys AA5754-O and AA5052-O, which are commonly used in marine applications. A systematic experimental design based on Taguchi's L16 orthogonal array was employed, incorporating four process variables: rotational speed (710–2000 rpm), traverse speed (20–80 mm/min), tool tilt angle (1°–4°), and pin profile (triangular, taper threaded, cylindrical threaded). Electrochemical corrosion tests (potentiodynamic polarization), microstructural analyses (optical and SEM), and statistical tools (ANOVA) were used to evaluate weld integrity and identify optimal parameters. Results demonstrate that defect-free joints with enhanced corrosion resistance are achieved using a triangular pin profile at 1400 rpm, 40 mm/min, and 1° tilt angle. In contrast, welds produced with a tapered and cylindrical threaded tools under lower travel speed and higher tilt angle exhibited reduced corrosion resistance. This study provides practical insights into optimizing FSW conditions to fabricate durable, corrosion-resistant joints for marine environments, addressing a key gap in current dissimilar alloy welding research.

## 1. Introduction

The ship building industry has recently demonstrated a strong interest in utilizing dissimilar aluminum alloys for maritime structures to reduce corrosion resistance and weight without increasing component costs [1]. Among the various aluminum alloy series, non-heat-treatable alloys such as AA5754 and AA5052 are well-suited for ship hull construction because of their corrosion resistance and excellent formability [2]. The 5xxx series aluminium alloys offer good corrosion resistance in marine environments and favorable welding characteristics. However, the high magnesium content in this series raises concerns about stress corrosion. Although these alloys exhibit a higher specific

[1]Mining and Metallurgical Engineering Dept., Faculty of Engineering, Assiut University, Assiut, Egypt. atef66@aun.edu.eg
[2]Manufacturing Engineering and Production Technology Department, Modern Academy for Engineering and Technology, Cairo, Egypt. MohamedAbuOkail@ gmail.com
[3]Mechanical Design and Production Engineering Department, Faculty of Engineering, Assiut University, Assiut, Egypt ibrahim.abdeldaiam@eng.aun.edu.eg
[4]Department of Mining and Metallurgical Engineering, Faculty of Engineering, Assiut University, Assiut, Egypt. Taghyan37@gmail.com

https://doi.org/10.21608/JESAUN.2022.124111.1104

strength compared to certain formable steel grades, weldability remains a significant challenge, especially with fusion welding techniques. Joining 5xxx aluminum alloys through conventional fusion welding methods is difficult due to issues like solidification cracks, shrinkage, and alloy segregation [3]. Conventional fusion welding techniques have been widely used for joining aluminum alloys. However, these methods often encounter significant challenges when applied to dissimilar aluminum joints, including excessive heat input, solidification cracking, porosity, and loss of mechanical properties due to microstructural degradation. These limitations are particularly critical in marine and aerospace applications, where joint integrity and corrosion resistance are paramount [4-5]. Recent studies [5-6] have highlighted the drawbacks of these conventional methods and emphasized the growing potential of solid-state techniques such as Friction Stir Welding (FSW) as a superior alternative for joining dissimilar aluminum alloys.

Additionally, welded joints typically display lower ductility and hardness, caused by the presence of a brittle inter-dendritic structure formed during the melting and re-solidification of the fused metal [7]. Therefore, FSW technology that is invented by The Welding Institute (TWI) in Cambridge is now widely employed to reduce several defects such as workpiece distortion, solidification cracking and gas porosity [8-9]. The significant increase of FSW licenses that were sold over the last decade is evidence of its growing popularity and stable expansion that makes it one of the most important inventions of the 1990's [10]. The FSW utilizes a non-consumable rotating tool with the requisite shoulder and pin size. The tool pin is inserted into plates to be joined as the tool rotates the heat is generated by friction among the tool and plates surfaces causes the weld plates to soften [11].

The tool's translation motion leads to the material to be pushed behind it. Owing to the solid state joining, defects can be reduced, and joint strength can be increased with equiaxed and fine grains formation [12]. Tool rpm, tool traverse speed, and tool geometrical characteristics, such as shoulder and pin diameter, are the key FSW parameters that influence weld quality [13]. Tian, et al. [14] studied a new forming method called constraint ring rolling (CRR) for making thin-walled conical cylinders with three ring ribs. They identified a defect called unreasonable material flow (UMF) in the single-pass process, which causes uneven rib formation. To fix this, they proposed a double-pass CRR method that forms two ribs first, then the third in a second step. This approach improves material flow, reduces forming force, and enhances the part's mechanical properties, making it more suitable for aerospace use despite slightly higher production costs. The study suggests the double-pass method as a reliable solution for high-performance ribbed components.

Abdelhady, et al. [6] investigated the optimization of friction stir welding (FSW) parameters for AA5754 aluminum alloy using the Taguchi method and grey relational analysis (GRA). Their goal was to enhance joint properties such as tensile strength, hardness, and impact toughness by fine-tuning key variables: rotational speed, welding speed, and tilt angle. The study identified the optimal welding conditions as 1000 rpm rotational speed, 60 mm/min welding speed, and a 2.5° tilt angle. These settings produced the best overall mechanical performance, achieving a tensile strength of 136 MPa, hardness of 85.25 HV, and impact toughness of 13 J. Rotational speed had the most significant influence on joint quality, followed by welding speed and tilt angle.

Improvements in hardness were mainly attributed to grain refinement in the weld zone caused by dynamic recrystallization during the FSW process. The research demonstrated that FSW is not only effective but also a cost-efficient method suitable for use in industries such as aerospace, automotive, and marine. Owis et al, [15] research successfully applied rotary friction welding with an external pressure tool to join aluminum alloy tubes edge-to-edge. Through experimentation with varying speeds and forces, they identified 1000 rpm and 30 kgF as the optimal parameters for achieving a maximum tensile dismantling force of 6160 N with a 4-minute welding time at a surface temperature of 200°C. This approach differs from previous studies by utilizing an external pressure tool applied perpendicularly to the rotation, whereas earlier methods relied on direct face-to-face pressure between the rotating and fixed parts. The study concludes that this modified rotary friction welding technique is effective for joining aluminum alloy tubes and suggests its potential applicability to other metals with necessary adjustments. Elmetwally et al. **[5]** study explored how different friction stir welding (FSW) speeds affect the joining and formability of pure aluminum and copper. They discovered that while high heat input during welding (achieved through high rotational speed and low travel speed) strengthens the joint, it also makes it less ductile due to work hardening. Conversely, lower heat input resulted in higher ductility. For applications where the welded part needs to be shaped further, the researchers recommend using moderate rotational speeds and higher travel speeds during FSW to avoid excessive hardening and maintain good formability. Essentially, the optimal welding parameters depend on the intended use of the joint: strength versus the ability to be formed.

Kilic et al. [16] found that process parameters significantly impact on the quality of weld joints, with key variables like tool design, rpm, welding speed, and axial force playing a crucial role. By adjusting these parameters, weld strength can be enhanced by decreasing defects. Çam et al. [17] compared two welding processes: FSW and friction stir spot welding (FSSW). They highlighted that FSW/FSSW provides distinct advantages over traditional fusion welding, particularly in terms of the materials it can join and the level of microstructural control achievable. FSW/FSSW is expected to see increased use in the future, particularly for hybrid structures involving multiple alloys that were once considered difficult or impossible to weld. Bella et al. [18] provided a comprehensive analysis of the primary process parameters and their impact on the mechanical properties and microstructure of a FSWed joint. Hui, et al [19] employed an Al-K2ZrF6 reaction system to prepare in-situ Al3Zr/AA6082 particle-reinforced aluminum matrix composites through an electromagnetic stirring melt reaction method, combined with FSW technology. The findings indicated that the optimal weld forming quality and tensile properties were obtained with welding parameters set at 14000 rpm and 50 mm/min. The impact of FSW parameters on the microstructure, mechanical properties and corrosion resistance of aluminum alloys have been the subject of several investigations. Khailiabad et al. [20] investigated the quality of FSW joints improves with increasing the pin diameter. Zhang et al [21] declared that the tensile strength of friction stir welded (FSWed) joints increases when the linear speed increases while the rotating speed decreases because of the grain size decreasing in the nugget zone. The effect of the tool tilt angle was analyzed by Krishna et.al. [22] and concluded that raising tilt angle led to minimizing the joint defect. Ugender [23] investigated the tool pin profile effect on the mechanical behavior, the result shows that threaded cylindrical pin generates sound weld in comparison to a taper cylindrical pin profile. Naik et al. [24] examined the effect of process parameters on corrosion behaviour and hardness. They found that using a hexagonal tool pin profile, a rotating speed of 1363 rpm, a welding speed of 715 mm/min, and an axial force of 8 kN resulted in improved corrosion resistance and hardness.

Aliha et al. [25] explored how tool welding and rotational velocities, along with the material used on the advanced side (AS) and retreating side (RS) of the weldment, affected the metallurgical and mechanical properties of the joint. They decided that using the stronger material AA7277-T6 on the advanced side led to higher microhardness and tensile strength. While several studies have explored the influence of individual FSW parameters on the mechanical or corrosion properties of similar or dissimilar aluminum alloys, limited work has focused specifically on dissimilar AA5052-O and AA5754-O alloys under varying pin profiles, tilt angles, and tool speeds—particularly in the context of corrosion behavior critical to maritime structures. Previous research has primarily addressed either mechanical strength or corrosion in isolation, without a comprehensive integration of microstructural analysis, electrochemical testing, and statistical optimization through the Taguchi method. Moreover, most existing studies do not explicitly optimize FSW parameters using a robust design of experiments (DOE) framework across multiple tool geometries for corrosion performance. The novelty of this work lies in its systematic approach to identifying optimal FSW process parameters using Taguchi L16 orthogonal arrays and ANOVA, and correlating them with corrosion resistance, microstructure refinement, and defect formation in AA5052-O/AA5754-O joints. This research uniquely provides guidance for fabricating corrosion-resistant, defect-free welds tailored for the harsh marine environment offering critical insights for lightweight and durable maritime structures. Swetha and Swetha, S., and Padhy [26] investigated the impact of various pin tool shapes on the FSW of AA-6061 T6 and AA-2014 T4. They executed FSW using cylindrical, square, and tapered pin shapes, keeping the rotational speed and feed rate constant. Kumar et al. [27] analyzed friction stir butt welds of dissimilar 6061 and 7075 Al alloys with different welding parameters, including tool rotational speed, tilt angle, and axial force, using a tool with a taper pin profile to determine optimal welding parameters. Prakash and Daso [28] optimized weld parameters, specifically tool speed, feed rate, displacement, and welding time, through Full Factorial Design, aiming to maximize impact strength, analyzed using statistical software to evaluate weld joint quality. Mohapatra and Sarangi [29] examined how the shape of the tool probe influenced the mechanical properties of the joint. They conducted experiments using five different rotational speeds for each tool shape. The results revealed that the square pin profile tool achieved the highest joint efficiency of 85%, followed by the triangular pin and cylindrical pin tools.

Ramana and Sanke [30] investigated FSW joining of AA 2021 and AA7075, employing High Speed Steel and Tungsten Carbide tools with varying hardness. They tested 1120, 1400, and 1800 rpm speeds and 30, 40, and 50 mm/min feeds, analyzing tensile strength and microstructure. HSS tool welds exhibited superior tensile properties over WC tool welds, which showed tunnelling effects. Kumar et al. [31] examined 6061 and 7075 Al alloy friction stir welds, varying tool rotational speed, tilt angle, and axial force with a tapered pin, testing twenty-seven 6.50 mm thick joints. They found impact strength increased with rpm to 900, then decreased at 1100, and similarly with axial force to 2.5 kN, decreasing at 3 kN; increased tilt angle raised impact strength. Process parameters significantly influence mechanical and corrosion properties of FSW joints [32, 33, 34].

Based on a literature review, the FSW process parameters have a major impact on the structural integrity and corrosion resistance of dissimilar aluminum alloys, particularly for applications in the shipbuilding industry. There have been limited research examining the mechanical and corrosion resistance of dissimilar FSW joints designed for maritime structures. From the previous survey it can be noticed that few studies have been done on the non-heat treatable aluminum alloys 5xxx series. This aluminum alloys series are used frequently in marine applications and a lot of studies are still needed to obtain the FSW characteristics and the effects of welding process parameters on microstructure and corrosion resistance of FSW joints obtained using aluminum alloys 5xxx series".

Therefore, this article aims to accomplish three key objectives. The first objective is to successfully fabricate defect-free dissimilar FSWed joints of AA5052-O and AA5754-O, specifically for use in maritime structures. The second objective is to identify the optimal and most reliable FSW process parameters using the Taguchi approach and ANOVA method. Finally, A key aim is to examine the structural properties and corrosion behavior of differently joined FSWed components of AA5052-O and AA5754-O for purposes of maritime structures.

## 2. Materials and methods

### 2.1. Experimental work

In this study, two different aluminum alloys AA5052-O and AA5754-O were chosen as the base materials based on their applications in maritime structures. The chemical composition and mechanical properties of aforesaid aluminum alloys are presented in Tables 1 and 2, respectively. The rolled plates of 4mm thickness of the base materials were cut by electrical discharge machine (EDM) into 160mm length and 100 mm width. After that steel wire brush and acetone were used to clean the surface of the plates by removing oxides.

The aluminum plates were securely clamped in place to form a butt joint configuration, as illustrated in Figure 1(a), which shows the friction stir welding (FSW) setup on a CNC milling machine. The welding process was carried out using a vertical CNC milling machine (Model XYZ-850, XYZ Machine Tools Ltd., UK), capable of programmable spindle speeds ranging from 100 to 8000 rpm and feed rates between 10 and 1000 mm/min. In the welding setup, the AA5052-O plate was positioned on the retreating side, while the AA5754-O plate was placed on the advancing side, as depicted in Figure 1(b), which displays the fixture and material arrangement for the FSW process. In this study, various FSW parameters were employed, including rotational speeds ranging from 710 to 2000 rpm, welding speeds from 20 to 80 mm/min, and tilt angles from 1° to 4°. A non-consumable hardened tool steel H13 with a hardness of 55 HRC was used to fabricate the stir welding tools. The materials and dimensions of the tool pin were selected based on the specific material and thickness of the aluminum alloy plates being joined. Different tool pin profiles were utilized: triangular, taper threaded, and cylindrical threaded, as illustrated in Figure 2. The detailed specifications of these tools are provided in Table 3. The tool shoulder was inserted into the clamped plates, which were secured to a specific fixture mounted on the milling machine table, as shown in Figure 1 (b).

A joint of dissimilar aluminum alloys AA5052-O and AA5754-O was produced through the FSW process using a vertical milling machine, as shown in Figure 1 (a), which has a table size of 1160 mm x 300 mm and a spindle speed range of 63-2800 rpm. The welding direction was maintained parallel to the rolling directions of the base materials. A single pass welding procedure was used to fabricate all the joints. Following the FSW process, samples for both microstructure analysis and corrosion testing were precisely cut using electrical discharge machining (EDM) to adhere to standard test dimensions. The samples underwent a meticulous surface preparation process, beginning with polishing using various grades of emery paper. This was followed by a final polish using a diamond compound with a particle size of 1 µm on a disc polishing machine. For corrosion testing, the surface preparation involved initial abrasion with 4000 grit silicon carbide (SiC) paper, followed by polishing with diamond paste down to 1 µm, using distilled water as a lubricant. Subsequently, the samples intended for microstructure analysis were etched with Keller's reagent to reveal the macro and microstructures, thereby elucidating the different FSW zones: the nugget zone (NZ), the thermomechanically affected zone (TMAZ), the heat-affected zone (HAZ), and the base metal regions.

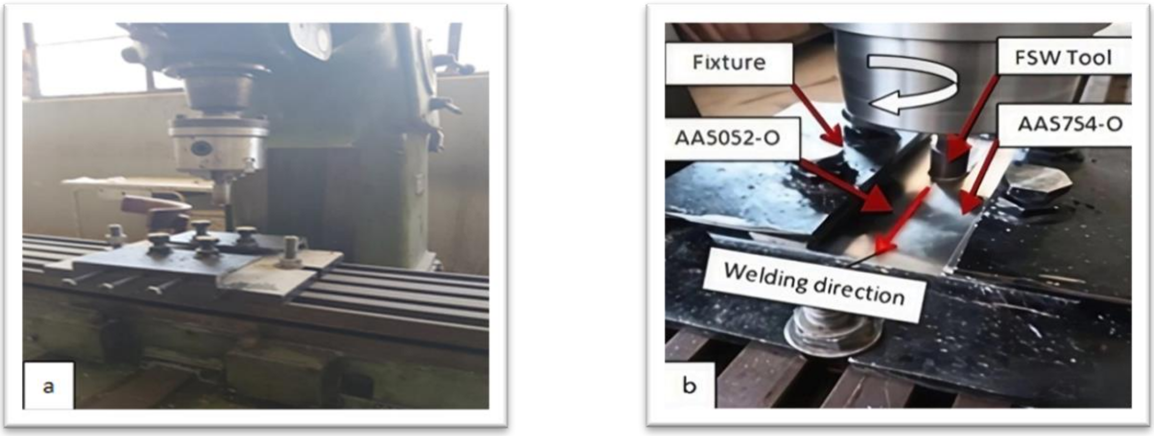


**Fig. 1: FSW setup (a) milling machine, and (b) fixture**

**Table 1. The chemical compositions of base aluminum alloys used**

| Materials | Mg | Si | Mn | Cr | Fe | Cu | Zn | Ti | Al |
|---|---|---|---|---|---|---|---|---|---|
| AA5052-O | 2.6 | 0.45 | 0.1 | 0.2 | 0.35 | 0.1 | 0.1 | 0.004 | 96.096 |
| AA5754-O | 3.17 | 0.61 | 0.03 | 0.37 | 0.26 | 1.53 | 0.2 | 0.15 | 93.68 |

**Table 2. The mechanical properties of base aluminum alloys used**

| Alloy | Ultimate tensile strength (MPa) | Yield strength (MPa) | Elongation (%) | Hardness (HV0.1) |
|---|---|---|---|---|
| AA5052-O | 190 | 79 | 22 | 47 |
| AA5754-O | 217 | 90 | 19 | 52 |

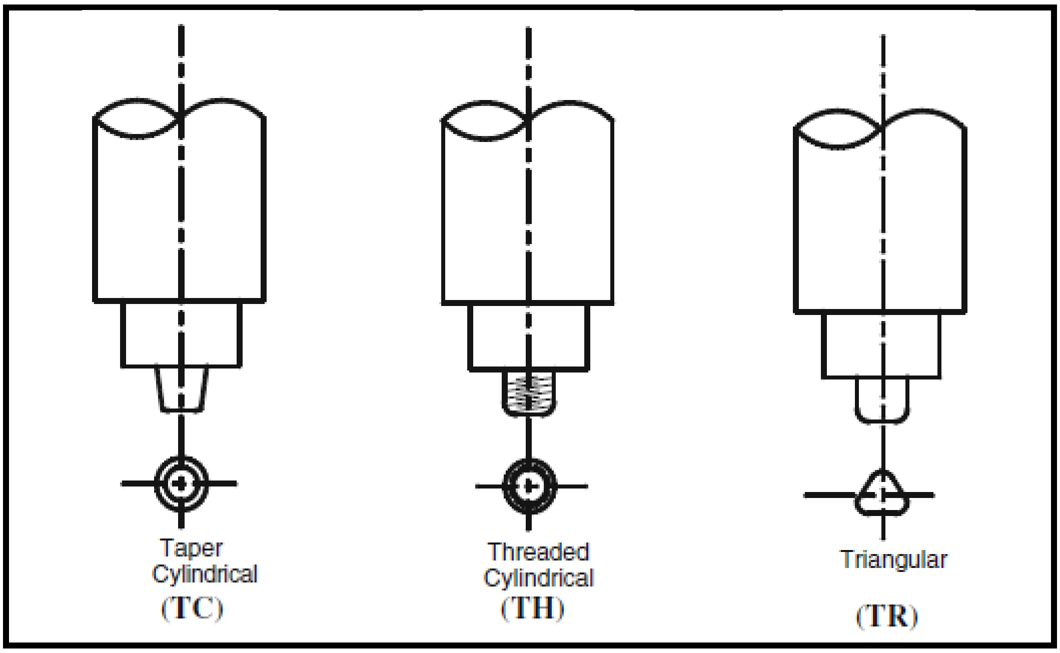


**Fig 2.: The FSW tools used in this study**

**Table 3: Tool specification and dimension**

| No | Tool design | Dimension |
|---|---|---|
| 1 | Shoulder diameter | 20 mm |
| 2 | Pin diameter | 6 mm |
| 3 | Pin length | 3.8 mm |
| 4 | Shoulder length | 40 mm |

Structural analysis, both macro and micro, was performed using a VERSAMET-3 light optical microscope with Clemex-Vision image analysis software and an FEI Quanta 3D 200i scanning electron microscope. Corrosion behavior was assessed by immersing welded samples in 3.5% NaCl. Linear polarization was conducted on 1 $cm^2$ x 3.5 mm samples, sectioned into base metal (BM), heat affected zone (HAZ), and weld metal (WM) via wire cutting. Metallographic preparation included sequential SiC grinding (100-1000 grit), 0.3 µm alumina and 1 µm diamond polishing, deionized water rinse, and acetone drying before electrochemical testing. A PGZ 100 potentiostat in 500 ml 3.5% NaCl at ambient temperature was used, with platinum auxiliary, calomel reference, and sample working electrodes. Steady-state OCP was measured, and potentiodynamic scans (-1 mV to +1 mV vs. OCP, 0.333 V/s) yielded corrosion currents. Tafel plots of potential vs. log I allowed calculation of corrosion current density (icorr) and potential (Ecorr). Corrosion rate (CR) was then calculated via Eq. (1) [35, 36]:

$$CR\ (mm/yr) = (0.00327 \times icorr \times eq.wt.)\ /D \qquad (1)$$

Where: icorr is current density, D is sample density, and eq.wt is equivalent weight. Post-corrosion, microstructure was analyzed by using a scanning electron microscope (SEM).

## 2.2. Design of experiments

The FSW process is conducted according to the Design of Experiments (DOE) table, which is based on the L16 orthogonal array using the Taguchi method from Minitab software. Rotational speed, linear speed, tool tilt angle, and pin profile were selected as input factors for this study. These factors and their limits were determined from preliminary experiments and a subsequent literature review, as well as machine capabilities, defining the parametric levels within the minima-maxima range. Table 4 details the welding parameters and their levels. Table 5 lists the FSW design parameters used in the present experimental work according to DOE.

**Table 4.Control parameters for FSW process**

| Parameter | Symbol | Units | Level | | | |
|---|---|---|---|---|---|---|
| | | | -2 | -1 | 0 | +1 |
| Rotational speed | RT | rpm | 710 | 1000 | 1400 | 2000 |
| Welding speed | WT | mm/min | 20 | 40 | 56 | 80 |
| Tilt angle | TA | degree | 1º | 2º | 3º | 4º |
| Pin profile | PP | - | cylindrical threaded | square | tapered threaded | triangular |

**Table 5: Experimental plan according to Taguchi L16OA**

| Specimen No. | Pin profile (PP) | Rotational Speed (RT) rpm | Welding Speed (WT) mm/min | Tilt Angle (TA) degree |
|---|---|---|---|---|
| 1 | Cylindrical threaded | 710 | 20 | 1 |
| 2 | | 1000 | 40 | 2 |
| 3 | | 1400 | 56 | 3 |
| 4 | | 2000 | 80 | 4 |
| 5 | Square | 710 | 40 | 3 |
| 6 | | 1000 | 56 | 4 |
| 7 | | 1400 | 80 | 1 |
| 8 | | 2000 | 20 | 2 |
| 9 | Tapered threaded | 710 | 56 | 1 |
| 10 | | 1000 | 80 | 2 |
| 11 | | 1400 | 20 | 3 |
| 12 | | 2000 | 40 | 4 |
| 13 | Triangular | 710 | 80 | 3 |
| 14 | | 1000 | 20 | 4 |
| 15 | | 1400 | 40 | 1 |
| 16 | | 2000 | 56 | 2 |

## 3. Results and discussion

### 3.1. Optical Microscopic Analysis of Welded Joints

The effect of tool pin profile and FSW parameters on the macro- and microstructure of dissimilar AA5052-O/AA5754-O welded joints was analyzed using optical microscopy (OM). Figures 3–5 illustrate the nugget zone (NZ) structures obtained under different tool geometries and welding conditions. The studied AA5xxx aluminum alloys contain high magnesium levels and additional elements such as Si, Fe, Cr, and Mn (Table 1), forming various intermetallic compounds may be including $Al_6Mn$, $Al_6MnFe$, $Mg_2Si$, and $Al_3Mg_2$. The morphology and distribution of these second-phase precipitates were observed to vary with welding conditions. Specifically, sample No. 3 (Figure 3) showed a lower density of intermetallics, while sample No. 13 (Figure 5) displayed large, bar-shaped precipitates up to 76 µm. Conversely, samples 14 and 15, welded using a triangular pin profile at optimal parameters, exhibited fine, nearly spherical precipitates evenly distributed within the NZ. Such microstructural refinement is widely associated with improved electrochemical stability due to minimized galvanic coupling and reduced initiation sites for localized corrosion.

These findings are consistent with previous research by Krishna et al. [22]and Naik et al. [24], who reported that uniform grain structures and fine precipitates significantly enhance corrosion performance in aluminum welds. Our results extend these conclusions by emphasizing the specific role of triangular pin profiles in achieving such beneficial microstructures in dissimilar AA5052/AA5754 joints—an area less explored in existing literature. This work thus adds valuable insight into the correlation between tool geometry and precipitate morphology in relation to corrosion behavior.

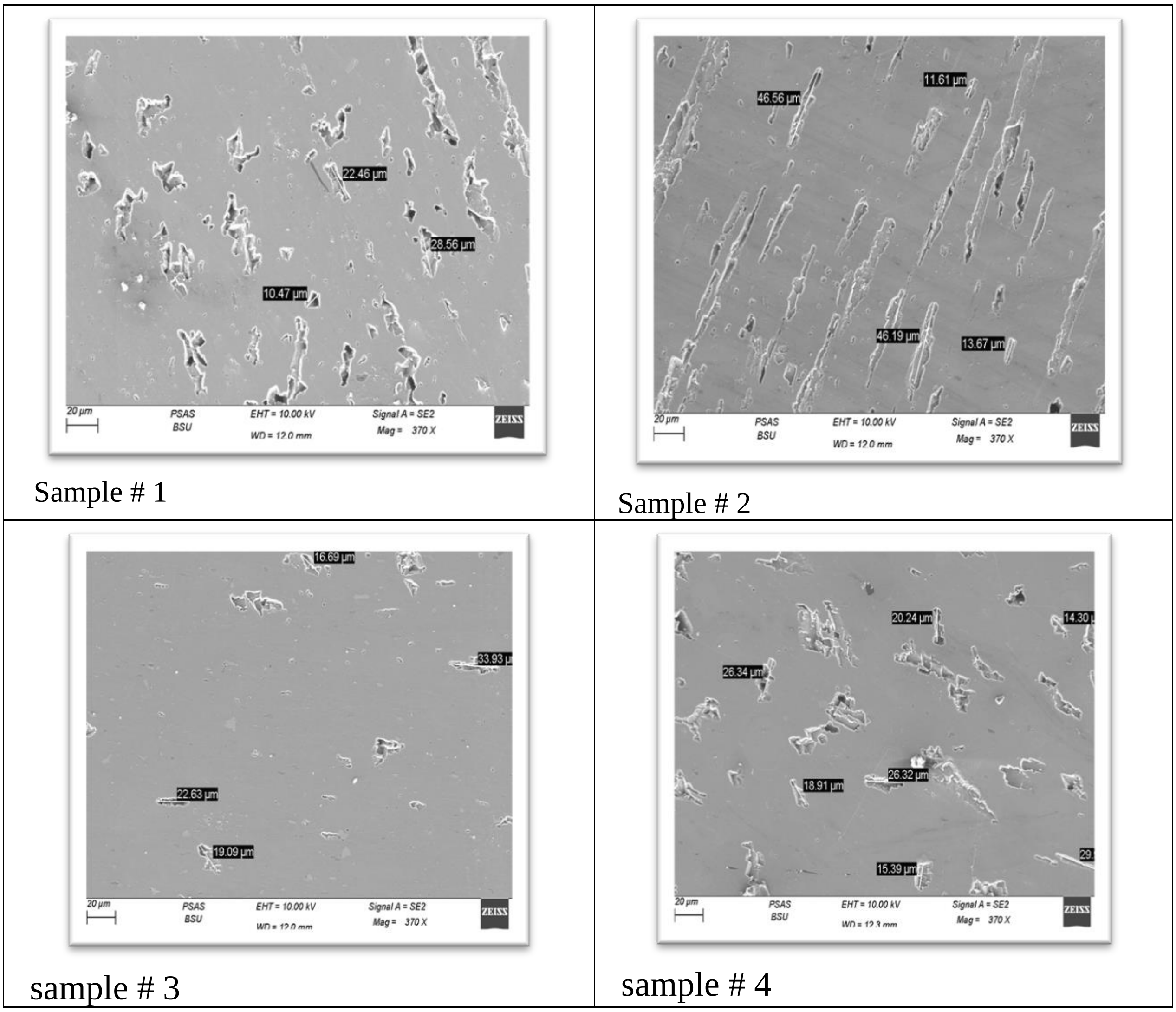

Fig. 3: OM micrograph of nugget zone (NZ) for FSWed joints for cylindrical threaded pin profiles.

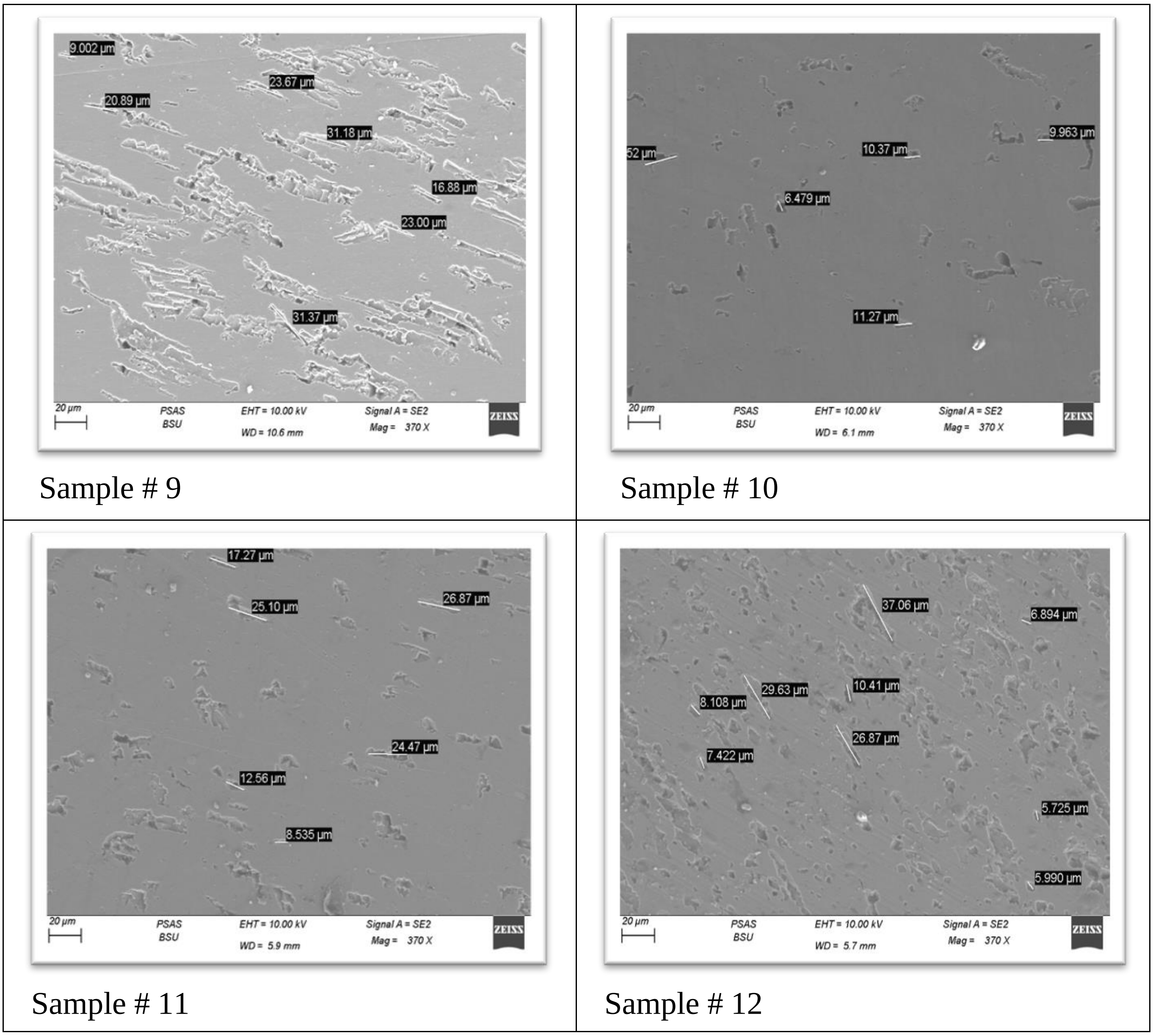


**Fig. 4: OM micrograph of nugget zone (NZ) for FSWed joints for tapper threaded pin profiles**

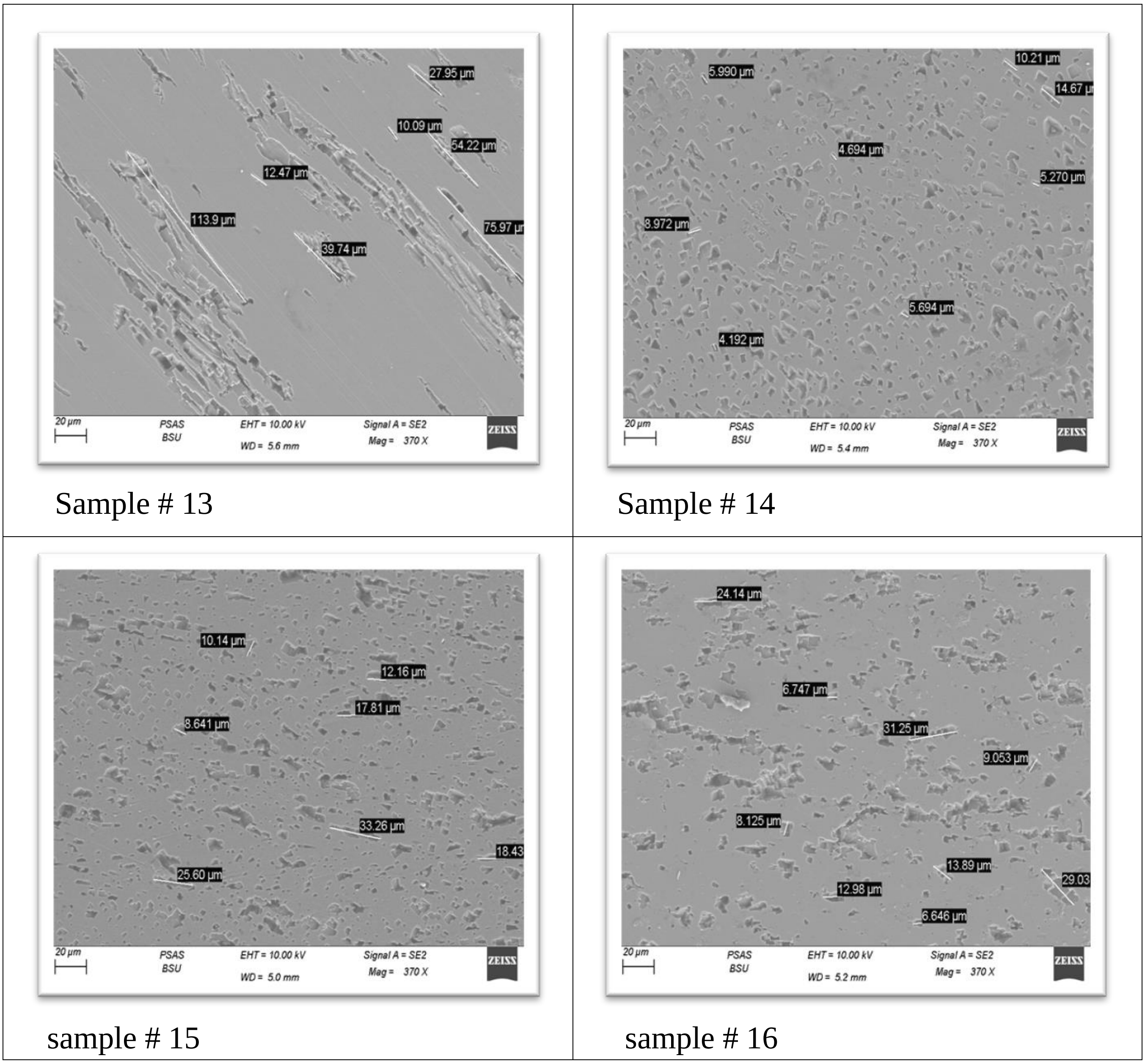


**Fig. 5: OM micrograph of nugget zone (NZ) for FSWed joints for triangular pin profiles.**

## 3.2. Corrosion Tests

### 3.2.1. Corrosion Behavior of FSWed Joints

Potentiodynamic polarization tests were carried out to evaluate the corrosion performance of the welded joints. The Tafel plots (Figure 6) and corresponding corrosion parameters (Table 6) show that tool geometry and process parameters significantly affect corrosion resistance. Joints welded with a triangular pin profile at 1400 rpm, 40 mm/min, and 1° tilt angle demonstrated the lowest corrosion rate and highest polarization resistance. This enhanced performance corresponds well with the refined and homogeneous microstructure observed in both OM and SEM analyses (Figures 5 and 9).

In contrast, joints produced with a tapered threaded pin profile (e.g., sample No. 11, Figure 4) exhibited the highest corrosion rate (CR = 0.083 mm/year) and more negative corrosion potentials, indicating inferior corrosion behavior. This is attributed to the presence of coarse elongated precipitates and less uniform material flow due to suboptimal stirring. SEM images (Figures 7–9) confirmed increased pitting and surface degradation in these samples, suggesting that inadequate thermal input and tool design contributed to microstructural heterogeneity and corrosion susceptibility. Our results strongly align with the conclusions of Naik et al. [24], who identified the importance of pin profile and thermal input on corrosion behavior. However, our findings differ from those of Ugender [23], who reported sound welds with threaded cylindrical pins. This discrepancy could arise from variations in alloy combinations, axial forces, or rotational speeds. By optimizing these parameters—specifically tool speed and tilt angle—we achieved superior corrosion resistance with the triangular pin, thereby contributing new comparative data to the literature.

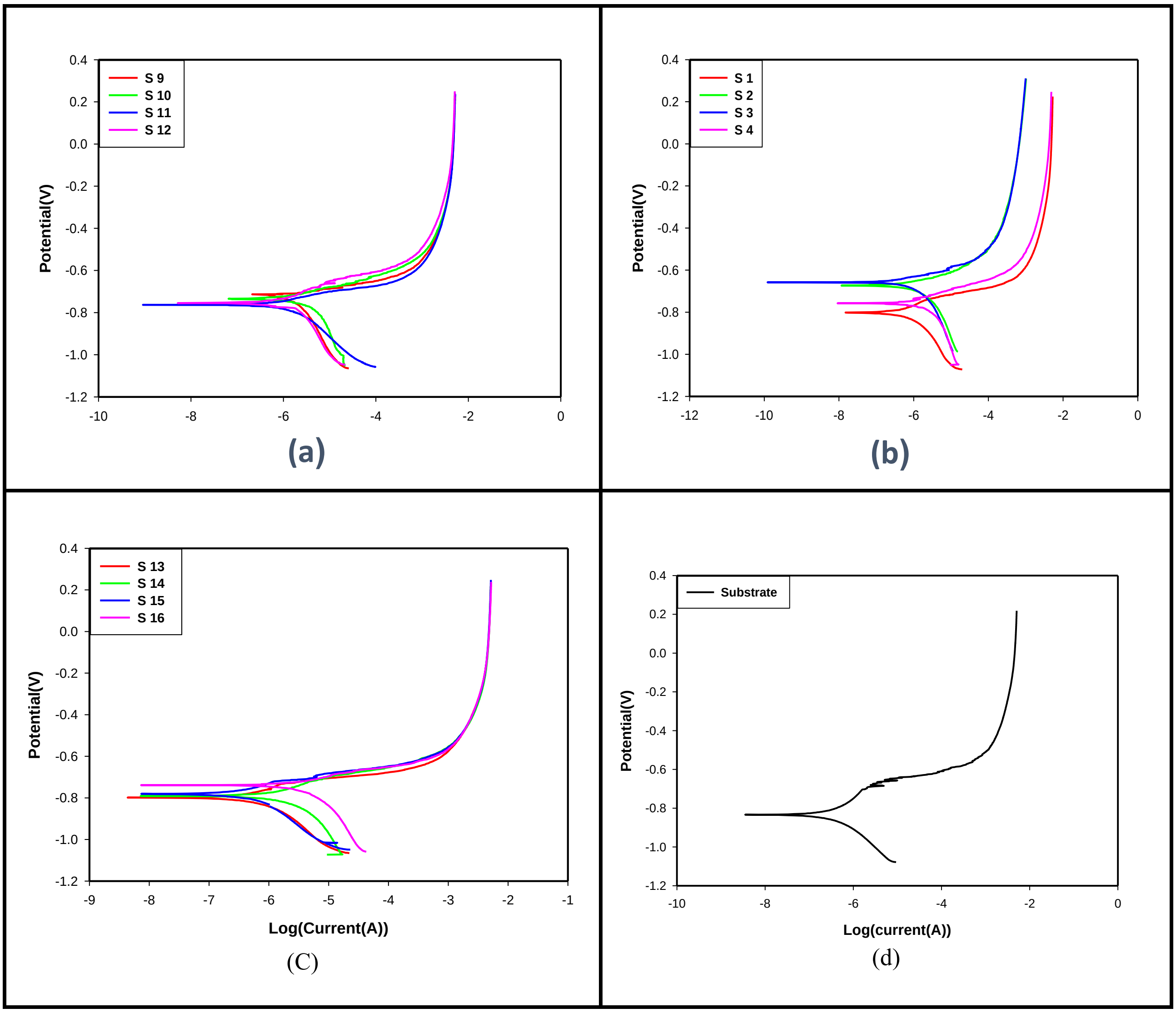


**Fig. 6: Potentiodynamic polarization curves of dissimilar FSWed joints for different pin profiles; (a) Cylindrical threaded, (b) Tapper threaded, and (c) Triangular (d) Substrate**

**Table 6: Corrosion rate polarization resistance (Ohm) E corr (V), J corer (A/cm2), Bc (V/dec) and Ba (V/dec).**

| Spec. No. | Corrosion rate (mm/year) | Polarization Resistance (Ohm) | E corr (V) | J corr (A/cm2) | Bc (V/dec) | Ba (V/dec) |
|---|---|---|---|---|---|---|
| 1 | 0.053 | 17209 | -0.803 | 4.91E-6 | 0.291 | 0.067 |
| 2 | 0.041 | 20090 | -0.674 | 3.74E-6 | 0.172 | 0.067 |
| 3 | 0.038 | 19930 | -0.659 | 3.54E-6 | 0.251 | 0.055 |
| 4 | 0.049 | 13094 | -0.758 | 4.50E-6 | 0.186 | 0.047 |
| 9 | 0.073 | 7917 | -0.715 | 6.77E-6 | 0.371 | 0.038 |
| 10 | 0.062 | 10864 | -0.737 | 5.69E-6 | 0.118 | 0.060 |
| 11 | 0.083 | 9725 | -0.764 | 7.61E-6 | 0.208 | 0.061 |
| 12 | 0.047 | 13287 | -0.755 | 4.32E-6 | 0.063 | 0.088 |
| 13 | 0.042 | 21667 | -0.800 | 3.88E-6 | 0.237 | 0.070 |
| 14 | 0.041 | 20832 | -0.792 | 3.79E-6 | 0.155 | 0.075 |
| 15 | 0.034 | 28779 | -0.782 | 3.15E-6 | 0.225 | 0.079 |
| 16 | 0.054 | 9617 | -0.740 | 4.99E-6 | 0.094 | 0.046 |
| **base metal** | 0.009 | 1.12E+5 | -0.834 | 8.90E-7 | 0.108 | 0.159 |

### 3.2.2. Corrosion Behavior of FSWed Joints vs. Base Metal (substrate)

The corrosion data reveal that the base metal **exhibits significantly superior corrosion resistance** compared to the welded joints:

- **Corrosion Rate:** The base metal displayed a very low corrosion rate of **0.009 mm/year**, while the corrosion rates of the FSWed joints ranged from **0.034 to 0.083 mm/year**, indicating a notable degradation in corrosion resistance post-welding.
- **Polarization Resistance (Rp)**: The base metal had the highest Rp value (**112,000 Ω**), whereas the joints showed much lower Rp values (**7,917 to 28,779 Ω**), indicating a higher tendency for corrosion.
- **Corrosion Potential (Ecorr):** The base metal exhibited the most noble potential at **−0.834 V**, while the FSWed joints had more negative potentials ranging from **−0.659 V to −0.803 V**, further indicating greater corrosion susceptibility in the welded zones..
- **Corrosion Current Density (Icorr):** The base metal had the lowest corrosion current density (**$8.90 \times 10^{-7}$ A/cm²**), in contrast to the FSWed joints (**$3.54 \times 10^{-6}$ to $7.61 \times 10^{-6}$ A/cm²**), confirming accelerated corrosion activity in the joints.

**Physical Explanation for Observed Variations:**

The significant difference in corrosion resistance between the base material and the joints is primarily attributed to microstructural and compositional changes introduced by the friction stir welding process:

1. **Microstructural Alteration**:

   The FSW process involves severe plastic deformation and frictional heating, which result in grain refinement, dynamic recrystallization, and phase transformations in the stir zone. These changes can disrupt the passive oxide layer and introduce microstructural inhomogeneities that serve as initiation sites for localized corrosion.

2. **Compositional Heterogeneity and Galvanic Coupling:**
   The mixing of dissimilar aluminum alloys (AA5052 and AA5754) in the weld zone leads to localized galvanic coupling between regions of different electrochemical potential. This drives preferential corrosion in less noble areas of the weld.
3. **Thermal Effects and Oxide Layer Breakdown**:
   Elevated temperatures during welding can degrade or locally dissolve the naturally protective aluminum oxide layer, reducing passivity in the welded region.
4. **Residual Stresses and Surface Conditions**:
   Welding introduces residual tensile stresses, which can further weaken the passive film and promote pitting or crevice corrosion under aggressive environments.

In contrast, the base metal (substrate), which remains unaffected by the thermal or mechanical impact of welding, retains its original homogeneous microstructure and stable passive film, resulting in markedly better corrosion resistance. These results confirm that the welding process negatively impacts the corrosion resistance of the material, and that FSWed joints are significantly more prone to corrosion than the unaffected base metal due to structural and compositional changes in the weld zone.

### 3.3. Taguchi Optimization and ANOVA Analysis

Signal-to-noise (S/N) ratios were calculated using the "smaller-the-better" criterion. The analysis showed that the triangular tool profile, 1400 rpm, 40 mm/min, and 1° TAO provided the most favorable corrosion resistance. ANOVA results confirmed that tool profile and rotational speed had the most significant influence on corrosion behavior, validating the model’s predictive capability and confirming convergence with the experimental findings.

### 3.4. SEM Analysis Before and After Corrosion

SEM examinations before and after corrosion testing (Figures 7–9) provided additional insights into the effect of tool geometry on microstructure and corrosion resistance. Joints fabricated with a triangular pin profile displayed minimal corrosion damage post-testing, limited to shallow and isolated pits. This is indicative of a stable oxide layer and uniform microstructure. In contrast, joints made with cylindrical and tapered pins suffered from deeper pits and more severe surface degradation, linked to irregular thermal distribution and less effective material stirring during welding.

The triangular pin tool enhanced plastic deformation and mixing, leading to uniform particle dispersion and refined grain structure. At 1400 rpm and 40 mm/min with a 1° tilt angle, the nugget zone contained uniformly distributed second-phase particles acting as dislocation barriers, thereby increasing mechanical integrity and reducing corrosion pathways. This observation aligns with the work of Krishna et al. [22] and Naik et al. [24], reaffirming the role of microstructural refinement in mitigating corrosion. Furthermore, our study supports the conclusions of Aliha et al. [25], who noted improved corrosion performance when stronger alloys were strategically positioned in the weld configuration. By employing a process that integrates optimal thermal control with tailored tool geometry, our results uniquely demonstrate that triangular pin profiles promote not only corrosion resistance but also consistent joint quality—extending previously reported findings and offering practical recommendations for marine-grade dissimilar aluminum welds.

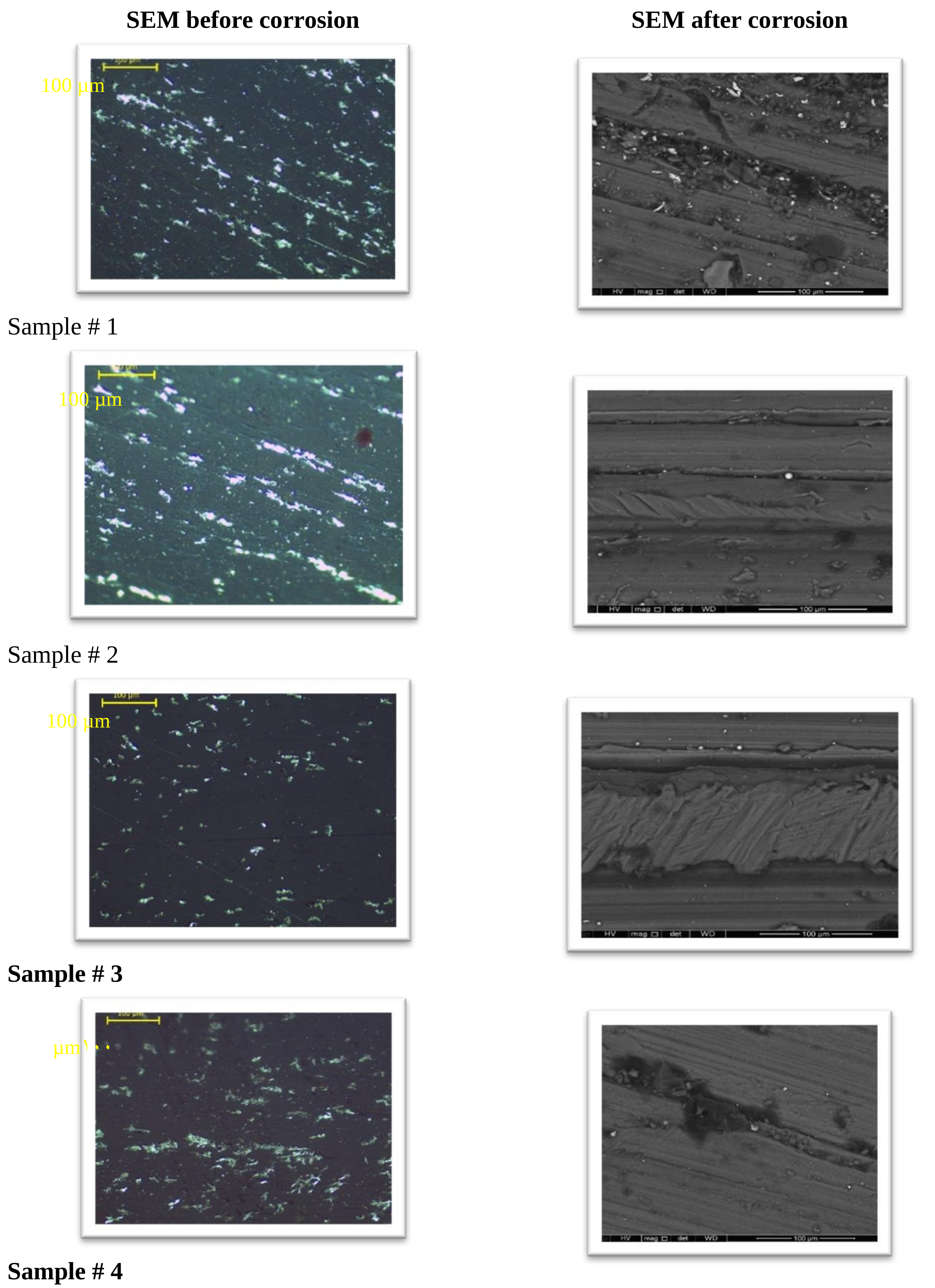


**Fig. 7: SEM images before and after corrosion for cylindrical threaded pin profile**

**SEM before corrosion** **SEM after corrosion**

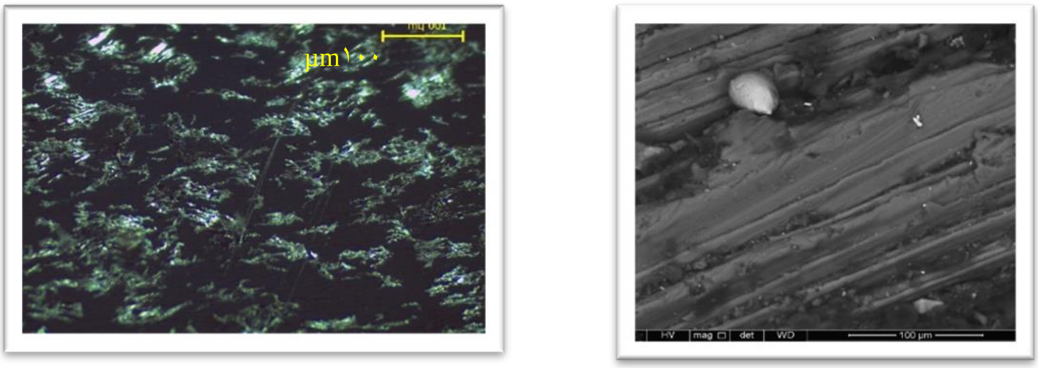

Sample 9

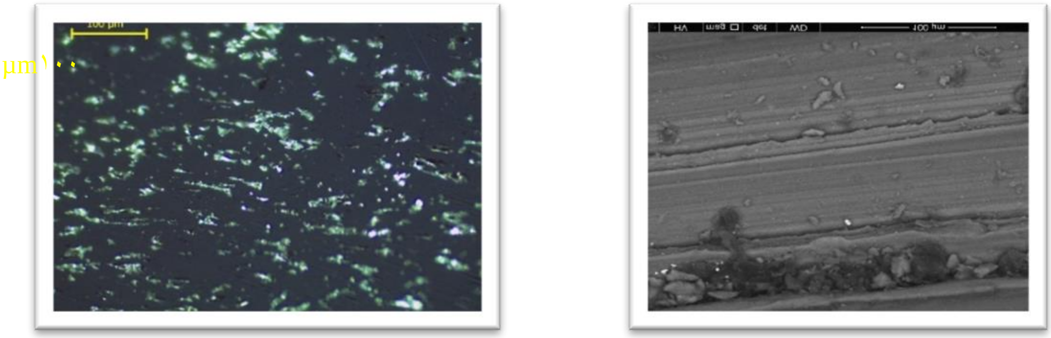

Sample 10

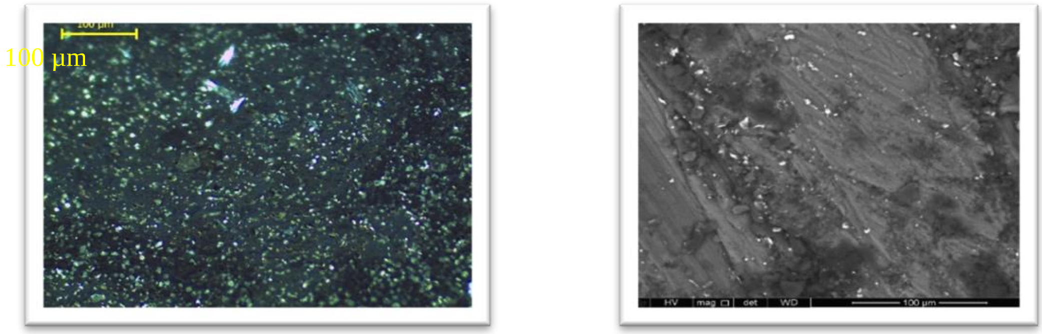


Sample 11

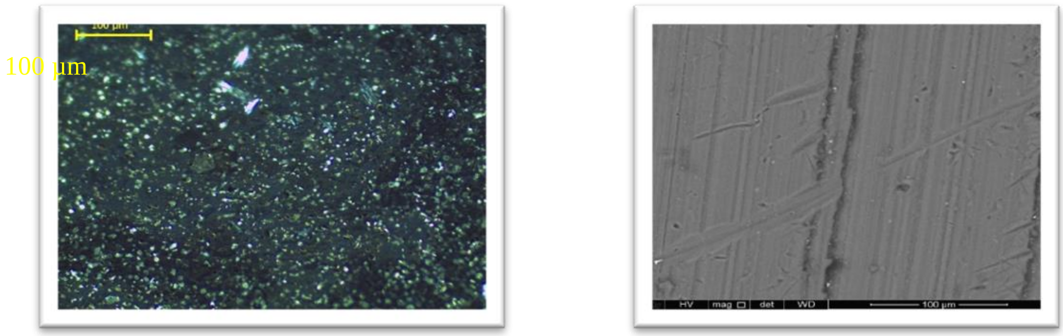


Sample 12

**Fig. 8: SEM images before and after corrosion for tapper threaded pin profile.**

| SEM before corrosion | SEM after corrosion |
|---|---|
| 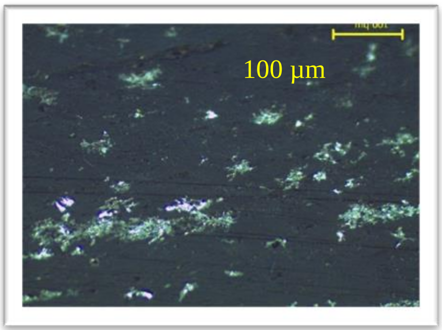  Sample 13 | 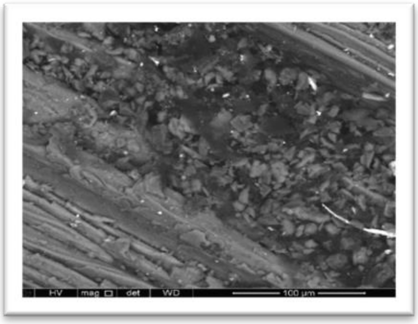 |
| 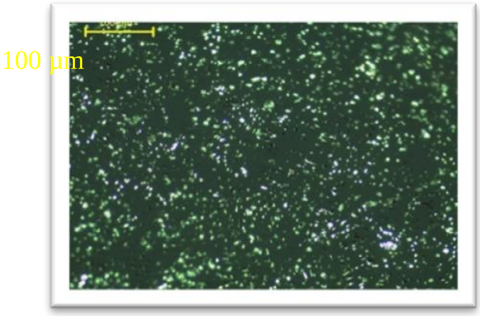  Sample 14 | 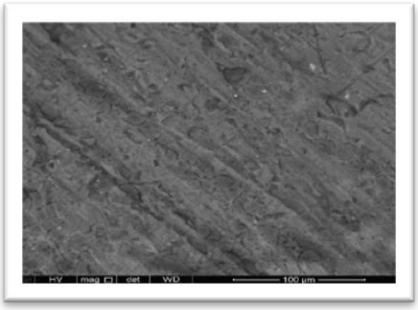 |
| 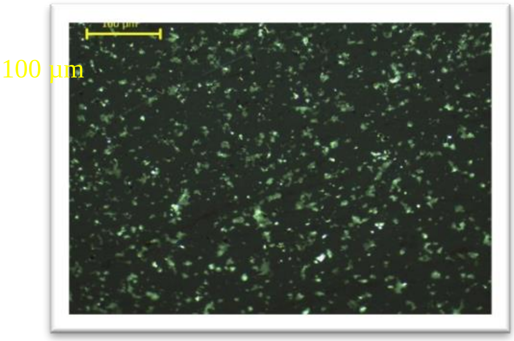  Sample 15 | 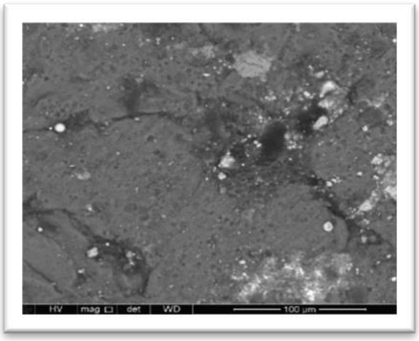 |
| 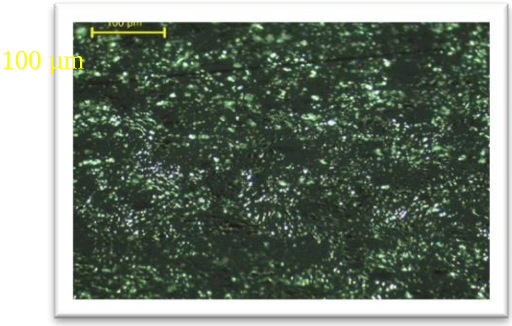  Sample 16 | 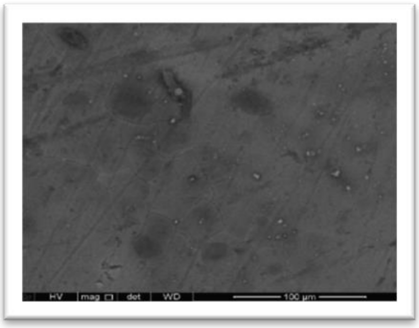 |

**Fig. 9: SEM images before and after corrosion for triangular pin profile.**

Overall, the results confirm that tool pin geometry and key FSW parameters critically influence the structural characteristics and corrosion resistance of dissimilar AA5052-O/AA5754-O welded joints. Our findings support several previously published studies while also offering new insights. The triangular pin profile consistently yielded the most refined microstructure and superior corrosion behavior. This study provides additional experimental evidence and optimization data, filling a gap in the literature regarding comprehensive microstructural and electrochemical characterization of FSWed dissimilar aluminum alloys for maritime applications.

## 4. Discussion

The microstructural evolution and corrosion performance of FSWed AA5052-O/AA5754-O joints were found to be strongly dependent on tool geometry and process parameters. The optical and SEM analyses revealed that the triangular pin profile consistently produced a refined microstructure and minimized second-phase precipitates. This agrees with findings by Krishna et al. [22] and Ugender [23], who reported that optimized pin geometry enhances stirring action and microstructural homogeneity, reducing weld defects.

The reduction in corrosion rate observed for welds created using the triangular pin profile (at 1400 rpm, 40 mm/min, and 1° tilt) can be attributed to the uniform distribution and morphology of precipitates. Similar improvements in corrosion resistance due to refined grain structures have been reported by Naik et al. [24] and Zhang et al. [21]. Their studies also emphasized the role of heat input and mechanical mixing in reducing galvanic coupling sites and pitting initiation zones, which supports the findings of the present work.

Conversely, welds made with cylindrical or tapered threaded profiles showed higher corrosion rates and more significant pitting, correlating with the presence of elongated or coarsely distributed intermetallics. These outcomes align with prior studies, such as Elmetwally et al. [6], which noted that excessive heat input or insufficient material flow can lead to coarse grain formation and reduced corrosion performance.

Moreover, the observed influence of rotational speed and traverse speed on the microstructure is consistent with Saleh et al. [6], who demonstrated that increased rpm enhances dynamic recrystallization but may also introduce thermal gradients that affect precipitate formation.

While previous research has investigated either corrosion resistance or mechanical properties individually, this study integrates both by linking microstructural evolution with electrochemical behavior under varied FSW conditions. This dual focus addresses a gap in the literature, particularly for AA5052-O/AA5754-O joints in marine applications.

In summary, the results validate existing knowledge on the effect of tool geometry and welding parameters while offering new insights specific to corrosion resistance in dissimilar 5xxx-series aluminum alloy joints. The findings suggest that using a triangular pin profile under optimized conditions provides a reliable approach for producing corrosion-resistant joints suitable for harsh marine environments.

## 5. Study limitations

This study focuses specifically on relatively thick aluminum alloy sheets (4.0 mm) of AA5052 and AA5754. It utilizes a single tool shoulder diameter and pin diameter, along with four types of tool pin profiles: cylindrical threaded, square, taper threaded, and triangular. Future research could explore a wider range of sheet thicknesses, pin profiles, pin diameters, and shoulder diameters. Additionally, it would be beneficial to examine the effects of post-weld heat treatment on the properties of friction stir welded joints.

## 6. Conclusions

Various methods, encompassing optical microscopy, scanning electron microscopy and potentiodynamic polarization testing, were employed to determine the welded joint integrity. Taguchi analysis and Analysis of Variance (ANOVA) were employed to determine the optimal process parameters using an L16 orthogonal array, which included four design factors and four parametric levels. The primary results and observations from the study led to the following major conclusions:

1. The optimal FSW parameters identified through Taguchi optimization and validated via ANOVA are now clearly linked to the lowest corrosion rate (CR = 0.034 mm/year) observed in Sample 15 using a triangular tool at 1400 rpm, 40 mm/min, and 1° tilt angle.
2. The correlation between coarse precipitate distribution (observed in OM/SEM images) and higher corrosion rates is now explicitly supported by microstructural and electrochemical data, particularly in welds produced with the tapered threaded profile.
3. We clarified how minimal and uniformly distributed precipitates (Samples 14 and 15) enhance corrosion resistance by supporting passive film formation—this is now explicitly tied to the potentiodynamic polarization results.
4. SEM analysis showing corrosion morphology after immersion in 70% $HNO_3$ for 24 hours is now better integrated into the discussion to support these findings.

The authors declare that there is no conflict of interest regarding the publication of this manuscript.

## References

[1] Abu-Okail, M., Ghafaar, M.A., Elshalakany, A.B., Mohamed S. Shiba, Ahmed Abu- Oqail & Mohammed Gamil "Investigation of Dynamic-Mechanical-Thermal Analysis of Innovative Hybrid Carbon/Glass Fibers Reinforced by GNPs and Al2O3 for Marine Structures", Fibers Polym 24, 4013–4029 (2023).

[2] Davis, J.R., "ASM Specialty Handbook: Aluminum and Aluminum Alloys,5th ed.", ASM International, Materials Park, 1993. https://www.asminternational.org/handbooks/-/journal_content/56/ 10192/ 06610G/ PUBLICATION (accessed Jun. 25, (2021).

[3] Birol, Y., and Kasman, S., "Effect of welding parameters on microstructure and mechanical properties of friction stir welded EN AW 5083 H111 plates", Mater. Sci. Technol., vol. 29, no. 11, pp. 1354–1362, Nov. 2013, Doi: 10.1179/1743284713Y.0000000280.

[4] J. P. Davim (ed.), Welding Technology, Springer Nature Switzerland AG, 2021 https://doi.org/10.1007/978-3-030-63986-0_1

[5] Hammad T. Elmetwally1, Hani N. SaadAllah, M.S. Abd-Elhady , Ragab K.Abdel-Magied, and Ayman Ali bd-Eltwab5, "Examination of the parameters effect on Al-Cu FSW welded butt joints using formability consent" Babylonian Journal of Mechanical Engineering Vol. 2024, 34–48, DOI: https://doi.org/10.58496/BJME/2024/006; ISSN: 3006-5410

[6] Saleh S. Abdelhady· Rehab E. Elbadawi· Said H. Zoalfakar" Multi-objective optimization of FSW variables on joint properties of AA5754 aluminum alloy using Taguchi approach and grey relational analysis", The International Journal of Advanced Manufacturing Technology (2024) 130:4235–4250 https://doi.org/10.1007/s00170-024-12969-2

[7] Peddavarapu, S., Raghuraman, S., Bharathi, R.J., Sunil, G.V.S., and Manikanta, D.B.N.S., "Micro Structural Investigation on Friction Stir Welded Al–4.5Cu–5TiB2 Composite", Trans. Indian Inst. Met., vol. 70, no. 3, pp. 703–708, Apr. 2017, Doi: 10.1007/s12666-017-1072-3.

[8] Lenin, A.W.A., Periyasamy, N., and George, L., "Influence of Interlayer Thickness (Zn) on the Properties of Al 7020 FSW Joints", Materials Research. 2016; 19(4): 817-823.

[9] Pathak, N., Bandyopadhyay, K., Sarangi, M., and Panda, S.K., "Microstructure and Mechanical Performance of Friction Stir Spot-Welded Aluminum-5754 Sheets", JMEPEG (2013) 22:131–144, Doi: 10.1007/s11665-012-0244-x.

[10] Krasnowski, K., Hamilton, C., and Dymek, S., "Influence of the tool shape and weld configuration on microstructure and mechanical properties of the Al 6082 alloy FSW joints", Arch. Civ. Mech. Eng., vol. 15, no. 1, pp. 133–141, Jan. 2015, Doi: 10.1016/j.acme.2014.02.001.

[11] Mishra, R.S., De, P.S., and Kumar, N., "Friction Stir Welding and Processing", Cham: Springer International Publishing, 2014. Doi: 10.1007/978-3-319-07043-8.

[12] Mishra, R.S., and Ma, Z.Y., "Friction stir welding and processing", Materials Science and Engineering R 50 (2005) 1–78.

[13] Çam, G., "Friction stir welded structural materials: beyond Al-alloys", Int. Mater. Rev., vol. 56, no. 1, pp. 1–48, Jan. 2011, Doi: 10.1179/095066010X12777205875750.

[14] Tian, D.; Han, X.; Lu, Z.; Zhuang,W.; Zhang, Z.; Deng, Z.; Hua, L., " Material Flow Control and Process Design in Constraint Ring Rolling of Thin-Walled Conical Cylinders with Three Ring Ribs", Materials 2025, 18, 1262. https://doi.org/10.3390/ma18061262

[15] Mohamed Sayed Owis, Samy Zein El-Abden, Ayman Ali Abd-Eltwab, and Karim and Mohammed Atia Abd Elkader Rotary Friction Welding of Aluminium Alloy Tube to Tube with Edge Using External Tool", JES, Vol. 52, No. 5, Sept. 2024 D O I: 10.21608/JESAUN.2024.258411.1298

[16] Kilic, S., Ozturk, F., and Demirdogen, M.F., "A comprehensive literature review on friction stir welding: Process parameters, joint integrity, and mechanical properties" , Journal of Engineering Research, Available online 6 September 2023,https://doi.org/10.1016/j.jer.2023.09.005.

[17] Çam, G., Javaher, V., and Heidarzadeh, A., "Advances in FSW and FSSW of dissimilar Al-alloy plates", January 2023, Journal of Adhesion Science and Technology, Volume 37, 2023.

**[18]** Bella, G.D., Favaloro, F., and Borsellino, C., "Effect of Process Parameters on Friction Stir Welded Joints between Dissimilar Aluminum Alloys: A Review", Metals 2023, 13, 1176. https://doi.org/10.3390/met13071176.

[19] Hui, L., Caizhi, S., Feng, W., Yuanpeng, Q., Chuying, L., Pinyi, X., Zatulovskiy, A., and Shcheretskyi, V., "Study on Microstructure and Mechanical Properties of Friction Stir Welding Joints of In-Situ Al3Zr/AA6082 Particle-Reinforced Aluminum Matrix Composites", Arch. Metall. Mater. 68 (2023), 3, 907-919.

[20] Khalilabad, M.M., Zedan, Y., Texier, D., Jahazi, M., and Bocher, P., "Effect of tool geometry and welding speed on mechanical properties of dissimilar AA2198–AA2024 FSWed joint", J. Manuf. Process., vol. 34, pp. 86–95, Aug. 2018, Doi: 10.1016/j.jmapro.2018.05.030

[21] Zhang, F., Su, X., Chen, Z., and Nie, Z., "Effect of welding parameters on microstructure and mechanical properties of friction stir welded joints of a super high strength Al–Zn–Mg–Cu aluminum alloy", Mater. Des., vol. 67, pp. 483–491, Feb. 2015, Doi: 10.1016/j.matdes.2014.10.055.

[22] Krishna, G.G., Reddy, P.R., and Hussain, M.M., "Effect of Tool Tilt Angle on Aluminum 2014 Friction Stir Welds", Global Journal of Research in Engineering: J General Engineering Volume 14 Issue 7 Version 1.0 Year 2014.

[23] Ugender, S., "Influence of tool pin profile and rotational speed on the formation of friction stir welding zone in AZ31 magnesium alloy", J. Magnes. Alloys, vol. 6, no. 2, pp. 205–213, Jun. 2018, Doi: 10.1016/j.jma.2018.05.001.

[24] Naik, D.B., Rao, C.H.V., Rao, K.S., Reddy, G.M., and Rambabu, G., "Optimization of Friction Stir Welding Parameters to Improve Corrosion Resistance and Hardness of AA2219 Aluminum Alloy Welds", Mater. Today Proc., vol. 15, pp. 76–83, 2019, Doi: 10.1016/j.matpr.2019.05.027.

[25] Aliha, M.R.M., Shahheidari, M., Bisadi, M., Akbari, M., and Hossain, S., "Mechanical and metallurgical properties of dissimilar AA6061-T6 and AA7277-T6 joint made by FSW technique", Int. J. Adv. Manuf. Technol., vol. 86, no. 9–12, pp. 2551–2565, Oct. 2016, Doi: 10.1007/s00170-016-8341-x.

[26] Swetha, S., and Padhy, C., "Tool pin profiles effect on mechanical properties of friction stir welding of dissimilar aluminium alloys", Materials today, Volume 92, Part 2, 2023, Pages 1092-1098, https://doi.org/10.1016/j.matpr.2023.05.132.

[27] Kumar, G.S.V.S., Kumar, A., Rajesh, S., Chekuri, R.B.R., and Ramakotaiah, K., "Optimization of FSW process parameters for welding dissimilar 6061 and 7075 Al alloys using Taguchi design approach", Int. J. Nonlinear Anal. Appl. 13 (2022) No. 1, 1011–1022.

[28] Prakash, M., and Das, A.D., “Investigation on effect of FSW parameters of aluminum alloy using Full Factorial Design” Mater. Today, p. 6, 2021.

[29] Mohapatra, S.S., and Sarangi, H., “Experimental investigation of tool probe shape and rotational speed on weld quality of friction stir welding of aluminum alloy” Mater. Today, p. 4, 2021.

[30] Ramana, G.V., and Sanke, N., “Evaluation of tensile and microstructure properties of AA2014 and AA7075 FSW weldments developed by HSS-10%Co and WC tools” Mater. Today, 6, 2021

[31] Kumar, G.S.V.S., Kumar, A., Rajesh, S., and Bhad, R.B., “Optimization of FSW process parameters for welding dissimilar 6061 and 7075 Al alloys using Taguchi design approach” Int. J. Nonlinear Anal. Appl. 13 (2022) No. 1, 1011–1022

[32] Mishra, R.S., and Ma, Z.Y., “Friction stir welding and processing”, Materials Science and Engineering R 50 (2005) 1–78.

[33] Bella, G.D., Favaloro, F., and Borsellino, C., “Effect of Process Parameters on Friction Stir Welded Joints between Dissimilar Aluminum Alloys: A Review, Metals 2023, 13, 1176. https://doi.org/10.3390/met13071176, https://www.mdpi.com/journal/metals

[34] Ramesha, K., Sudersanan, P.D., Santhosh, N., and Jangam, S., “Corrosion Characterization of Friction Stir Weld Joints of Dissimilar Aluminum Alloys”, Chennai, India, DOI 10.4108/eai.16-5-2021.2304097

[35] Elangovan, K., and Balasubramanian, V., “Influences of tool pin profile and welding speed on the formation of friction stir processing zone in AA2219 aluminum alloy”, journal of materials processing technology 200 (2008), 163- 175.

[36] Terra, C.S., and Silveir, J.L.L., “Models for FSW forces using a square pin profile tool”, Journal of Manufacturing Processes 68 (2021) 1395–1404.